A Numerical Study of Moisture and Ionic Transport in Unsaturated Concrete by Considering Multi-ions Coupling Effect

Meng, Zhaozheng; Zhang, Yufei; Chen, Wei kang; Fu, Chuan qing; Xiong, Qing Xiang; Zhang, Cheng lin; Liu, Qing feng

Important note
To cite this publication, please use the final published version (if applicable).
Please check the document version above.

A Numerical Study of Moisture and Ionic Transport in Unsaturated Concrete by Considering Multi-ions Coupling Effect

Zhaozheng Meng[1,2,5] · Yufei Zhang[3] · Wei-kang Chen[1,2] · Chuan-qing Fu[4] · Qing Xiang Xiong[1,2] · Cheng-lin Zhang[1,2] · Qing-feng Liu[1,2]

Abstract

Understanding the transport mechanisms within unsaturated porous media is essential to the durability problems associated with cement-based materials. However, the involvement of multi-ions electrochemical coupling effect, especially under unsaturated condition makes the transport mechanisms even more complex. In this study, the moisture and multi-ionic transport in unsaturated concrete have been modeled in three-dimensional cases. The contribution from both water vapor and liquid has been considered in moisture transport. By adopting the constitutive electrochemical law, the electrostatic potential induced by inherent charge imbalance was calculated. With parameter calibration, the numerical results agreed well with the experimental data, proving the validity of the presented model. Results from a parametric analysis showed that neglecting multi-ions coupling effect will lead to an underestimated chloride concentration, and saturated degree has an obvious impact on the coupling strength among different ions. In addition, the existence of coarse aggregates will not only block mass transport but also make the discrepancies between two-dimensional model and three-dimensional model results more obvious. Other findings which have not been reported in existing studies are also highlighted.

✉ Qing-feng Liu
liuqf@sjtu.edu.cn

1   State Key Laboratory of Ocean Engineering, School of Naval Architecture, Ocean and Civil Engineering, Shanghai Jiao Tong University, Shanghai, China

2   Shanghai Key Laboratory for Digital Maintenance of Buildings and Infrastructure, Shanghai, China

3   Department of Civil and Environmental Engineering, Faculty of Science and Technology, University of Macau, Macau, China

4   College of Civil Engineering and Architecture, Zhejiang University of Technology, Hangzhou, China

5   Microlab, Faculty of Civil Engineering and Geosciences, Delft University of Technology, 2628 CN Delft, The Netherlands

Article Highlights

- The coupled moisture and multi-ionic transport process has been modeled in three dimensions for the first time.
- The anomalous moisture transport has been considered by time-dependent water permeability.
- The higher saturation degree has been found to amplify the multi-ions coupling intensity in porous media.
- The model heterogeneity and dimension should be properly considered to obtain more accurate numerical result.

1 Introduction

Concrete is the most widely used construction material in the world because of its availability and good performance (Song et al. 2008; Bertolini and Redaelli 2009). However, the durability deterioration of concrete structures is a very prominent problem (Tang and Gulikers 2007; Fu et al. 2016), which is attributed to the penetration of harmful substances such as chloride ions due to the porous nature of concrete (Savija et al. 2014; Ukrainczyk and Koenders 2014). When concrete is fully saturated, chloride transport is mainly governed by diffusion (Tang 2008). However, considering the fact that most of the existing concrete structures are rarely saturated (Baroghel-Bouny et al. 2011; Zhang et al. 2012), the bulk movement of moisture in porous medium will make the ionic transport behavior much more complicated compared to the saturated cases (Bao et al. 2020; Chen and Liu 2021). In addition, because of the different diffusivities and charges of each ionic species, a charge imbalance inside concrete pore solution can be induced, which will produce an electrostatic potential and in turn influence the ionic transport behavior (Johannesson et al. 2007; Elakneswaran et al. 2010). Thus, investigations on the coupled mass transport of moisture and multi-ions in unsaturated concrete are of great significance for understanding the durability issues of concrete and more accurately predicting their service life (Wang et al. 2018; Hou et al. 2019).

When concrete is unsaturated, water tends to intrude into it mainly through capillary absorption (Bažant and Najjar 1972). This water intrusion process is very complex since the moisture diffusivity is dependent on various influence factors and also the intrinsic microstructures of concrete (Hall 1989; Garbalinska et al. 2010; Xiong et al. 2023). Several advanced experimental methods were conducted to monitor the moisture transport in cementitious materials (Mercado-Mendoza et al. 2013; Zhang et al. 2017), and some other studies have also been carried out to determine the moisture diffusivity in different forms (Wong et al. 2001; Zhou 2014). Besides, in terms of the influence of moisture transport on ionic transport, it can be mainly reflected from two aspects. Firstly, ions dissolved in water solution can be transported into concrete because of convection, which is much faster than the ionic diffusion in saturated concrete (Zhang et al. 2018). In addition, the moisture content and moisture distribution in the pore network can have profound impacts on ionic diffusivity (Guimaraes et al. 2011; Tong et al. 2023). Vera et al. (2007) and Climent et al.

(2002) proposed test methods to measure chloride diffusivity of unsaturated concrete with different controlled water content. Similarly in another test (Nielsen and Geiker 2003), chloride diffusivity was measured under relative humidity levels of 65% and 85%. The coupled transport of water and chloride in cement mortars was analyzed by Černý et al. (2004) with an initial relative humidity of 45%, and ionic binding was taken into account in their study. More recently, Homan et al. (2016) developed a new experimental method to characterize the moisture-chloride interaction in non-saturated concrete.

The above-mentioned experimental works investigated the ionic transport in unsaturated concrete based on different preconditions and thus it is difficult to unify the test results. Meanwhile, because of the coupling effect among different influence factors, it is also tricky to analyze the individual action of each factor only by means of experiment. Consequently, more and more researchers have attempted to adopt numerical modeling techniques to solve the moisture and ionic transport. In terms of moisture transport, Caggiano et al. (2018) developed a mesoscale approach to simulate the moisture movement, and the influence of microstructure morphology of cementitious material has been considered. Then, Singla et al. (2022) investigated the impact of crack on moisture transport by using the lattice model. As for the coupled moisture and chloride transport, Meijers et al. (2005) studied the chloride ingress process in concrete under drying-wetting cycles, and the carbonation effects were also taken into account. Then, based on the previous diffusion-based models, Oh and Jang (2007) proposed an extended prediction model, which considers multiple transport processes including diffusion, convection and chloride binding. By applying the multiscale lattice Boltzmann-finite element model, Zhang et al. (2014) investigated the effect of water saturation degree on ionic diffusivity in unsaturated concrete. Liu et al. (2021) developed a numerical model to investigate the effect of water vapor on chloride transport, and it showed that the drying-wetting ratio has an obvious influence on the chloride concentration distribution pattern. Recently, by considering multiple modal of pore size distributions, Tong et al. (2024a) established an improved model for predicting moisture transport features in unsaturated cementitious materials.

As mentioned earlier, there are various positively and negatively charged ionic species in concrete pore solution, and the electrochemical interaction among different species also influences the ionic transport behaviors (Khitab et al. 2017; Patel et al. 2021; Liu et al. 2023a, b). This action is regarded as the multi-ions coupling effect among different ionic species (Yang et al. 2019). At first, researchers tended to characterize the coupling action among multiple ions in saturated medium based on the hypothesis of null current or electro-neutrality (Li and Page 2000; Frizon et al. 2003). However, it was founded that this kind of assumption is not a constitutive law but only a mathematical approximation that may cause numerical inaccuracy (Liu et al. 2012). Most importantly, Johannesson et al. (2010a; b) modified the description of multi-ionic coupling based on the real electrochemical interaction among different species and their results were proved to be more accurate than those based on the electro-neutrality assumption. Liu et al. (2015; 2018) further investigated the multi-ions coupling effect when external electric field existed, and results showed that the multi-ions coupling effect has a significant impact on ionic migration speed, and the influence also depends on the charge characteristics. In addition to the influence of multi-ions coupling, with the rapid development of computational modeling techniques and also the deeper understanding on the chloride binding and reactive transport mechanisms, much more advanced models have been proposed (Liu et al. 2023a, b). Hosokawa et al. (2011) proposed a multi-ions reactive transport model and highlighted the importance to include the chemical aspects in a detailed way to model and understand the chloride penetration and reaction mechanisms. Apart from the interaction

between ionic constituents and complexes solid cement hydrates, the composition of the initial and evolving concentrations of the ionic species in the concrete pore solution (such as the existence of sulfate ions) will also influence the transport behavior of ionic species (Hosokawa et al. 2012; Zhang et al. 2021). More recently, the multi-ions coupling strength under combined chloride-sulfate attack in cementitious materials was also investigated, and it was reported that the multi-ions coupling has a non-negligible effect on the competitive binding mechanism between chloride and sulfate ions (Meng et al. 2024).

So far, the individual effect of water convection and multi-ions coupling on ionic transport has been summarized in literature review. The coupled effect of these two actions on chloride transport in unsaturated concrete needs to be further studied. Samson et al. (2005; 2007) studied the coupled transport of moisture and multi-ions in unsaturated porous media by using the homogenization technique, which was proved to be a powerful mathematical tool. Based on the mixture theory and single phase system, Johannesson et al. (2003, 2009) implemented an efficient finite element method to solve the nonlinear problem of ionic diffusion and moisture movement in a porous material. Further, with account to the sorption hysteresis, a model for ionic transport coupled to moisture transport was presented by Jensen et al. (2015) and their study showed the sorption hysteresis would influence the ionic concentrations. Recently, Na and Xi (2019) applied parallel computing method to obtain a faster convergence as compared with other multi-ions transport models in unsaturated conditions. However, the moisture was considered as a single phase, and the impact of multi-ions coupling effect was also not essentially discussed.

The above literature review indicates that although chloride ingress in unsaturated concrete has attracted much attention, relatively a few studies are available regarding multi-species ionic transport. Limited researches are available regarding the coupled transport of moisture and multi-ions, and most of them treat concrete/cement as a one-dimensional homogeneous material. Based on the remarkable progresses and solid foundations from previous studies, the present work aims to explore the coupled transport of not only moisture and chloride, but also multiple ionic species in unsaturated concrete, in which concrete is treated as a heterogeneous material in three dimensions. In such a case, the electrostatic potential induced by the charge imbalance is carefully studied and the effects of unsaturated conditions on multi-ions coupling effect are presented. Some important influencing factors (heterogeneous characteristic, initial saturation and ionic interaction, etc.) during the transport process are also discussed in details.

2 Mass Transport in Porous Media

The schematic diagram of the coupled moisture and multi-ionic transport mechanisms in concrete is shown in Fig. 1 under multiple scales. Generally, in terms of concrete structures serving in coastal areas and exposed in tidal zones, the bulk movement of water will aggravate the penetration of harmful substances and provide necessary conditions for the initiation of durability problems such as steel corrosion, which will eventually lead to cracking and even spalling of concrete cover (Cai and Liu 2023). Moreover, accompanied with the moisture transport, deleterious ions dissolved in pore solution will penetrate into the concrete much more quickly through the convection
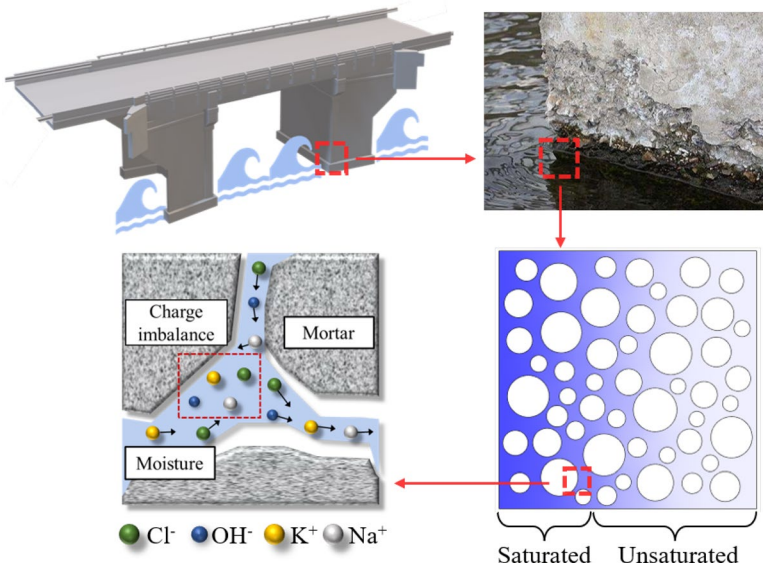
Fig. 1 Schematic diagram of the mass transport process in porous medium at different scales

effect (Xiong et al. 2024). Meanwhile, a charge imbalance can be induced because of various diffusivities of different ionic species, which will introduce an electrostatic potential inside concrete pore solution, and in turn result in the electromigration phenomenon in ionic transport. Consequently, multiple processes including diffusion, convection and migration need to be considered in the multi-ionic transport. Given the fact that the entire process occurs under an unsaturated condition, the moisture transport model should be firstly established to determine the saturation condition during the exposure time. Subsequently, multi-species ionic transport process driven by different factors will be formulated, and the influence of moisture transport on ionic transport behavior will also be considered.

2.1 Moisture Transport

As for porous materials such as concrete, moisture can serve as the transport medium of aggressive agents in concrete pore network (Tong et al. 2024), and many durability problems are associated with moisture transport in porous medium. By assuming that the ambient atmospheric pressure is constant, moisture transport in porous materials like concrete can be sufficiently characterized thorough the two-phase modeling, that is, liquid water transport driven by hydraulic pressure gradient and vapor diffusion driven by the vapor content gradient. Therefore, saturation degree, θ, can be expressed based on the mass conservation law as

$$\frac{\partial \theta}{\partial t} = -\frac{1}{\rho_1 \phi} \nabla \cdot \left(J_1 + J_g \right) \tag{1}$$

where ρ_1 (kg/m^3) represents the liquid water density; φ represents the porosity; J_1 (kg/(m^2 s)) and J_g (kg/(m^2 s)) represent the liquid water flux and vapor flux, respectively.

The thermodynamic equilibrium between the liquid water and vapor in pore space should also be properly considered. In this study, the equilibrium is related by Kevin's law which can be expressed as

$$P_c = -\frac{RT\rho_l}{M_w} \ln RH \tag{2}$$

where P_c (Pa) represents the capillary pressure defined as the difference between the gas and liquid pressure (i.e., $P_c = P_g - P_l$), and P_g and P_l represent the gas pressure and liquid water pressure, respectively; P_g; R (J/(K·mol)) represents the ideal gas constant; T (K) is the absolute temperature which has been taken as the room temperature (293.15 K) in this study; M_w (kg/mol) is the molar mass of water; RH represents the relative humidity. For cementitious materials, the capillary pressure can be depicted by the water vapor sorption isotherm. In this study, the well-known van Genuchten equation (Van Genuchten 1980) has been adopted, which can be expressed as

$$P_c = \alpha \left(\theta^{-1/m} - 1 \right)^{1-m} \tag{3}$$

where α and m are fitting parameters which can be quantified by fitting the experimentally tested water vapor sorption isotherms (Zhang et al. 2016; Zhang and Angst 2020).

As for liquid water, the modified Darcy's law can be adopted to depict its transport behavior in unsaturated porous materials, which can be expressed as

$$J_l = -\rho_l \frac{k_{rl} K_l}{\mu_l} \nabla P_l \tag{4}$$

where μ_l (Pa s) represents the dynamic viscosity of liquid water; P_l (Pa) represents the liquid pressure; K_l represents the permeability of liquid water, and k_{rl} represents the relative liquid water permeability. Since it is difficult to directly measure the liquid water permeability under different relative humidity, the relative liquid water permeability k_{rl} is assumed to be as a function of saturation degree. Therefore, an analytical function has been proposed based on van Genuchten–Mualem equation in Eq. (3), which has been called as the van Genuchten–Mualem (VGM) model (Van Genuchten 1980)

$$k_{rl} = \theta^l \left[1 - \left(1 - \theta^{1/m} \right)^m \right]^2 \tag{5}$$

where m is the same fitting parameter as mentioned in Eq. (3); l is the critical tortuosity which was commonly adopted as 0.5 for soil. According to the study by Monlouis-Bonnaire and Perrin (2004), 5.5 was suggested for cementitious materials, which has also been adopted in this study. However, it should be noted that this value would vary for different porous materials and even different for cement pastes with different mix proportions, so parameter quantification by fitting the experimental measurement is recommended in the future studies.

In addition, recent studies have also reported that the water permeability K_l is also time dependent, and the water absorption will deviate from the square root of time law in the later adsorption stage. Therefore, the time-dependent nature of local water permeability was expressed by the exponential relationship firstly proposed by Hall (2019) as

$$K_l = K_1 + \left(K_0 - K_1 \right) \exp \left[-\left(t_c / \tau \right)^\gamma \right] \tag{6}$$

where it can be seen that the water permeability is expected to decay from the initial value of K_0 to the ultimate value of K_1 during the time period of τ; γ is the exponent; and t_c is the contact time which can be defined as the difference between the current time and the moment when the moisture content at a given space begins to change. It therefore suggests that the contact time t_c and also the water permeability are related to both time and space location.

In terms of the vapor flux, it can be depicted by a diffusion-like equation as

$$J_g = -D_v^{\text{eff}} \nabla \rho_v \tag{7}$$

where ρ_v (kg/m^3) represents the vapor density, and D_v^{eff} (m^2/s) represents the effective diffusion coefficient of vapor, which can be determined by various methods. In this study, the effective diffusion coefficient of water vapor is characterized as follows according to the study by Millington and Quirk (1961)

$$D_v^{\text{eff}} = \frac{(1 - \theta)\phi}{\sigma} D_v^0 \tag{8}$$

$$\sigma = [(1 - \theta)\phi]^n \phi^2 \tag{9}$$

where σ is a correction factor charactering the blocking effect caused by liquid and solid phase intrusion, porous tortuosity during the vapor diffusion process; D_v^0 is the free vapor diffusivity in the air which can be taken as 2.45×10^{-5} m^2/s under room temperature (293.15 K) according to (Li and Li 2013); coefficient n was initially determined as $-7/3$ by Millington and Quirk for soils. However, for cementitious materials whose porosity may be smaller than the soils, Thiery et al. (2013) suggested to take n as -3.74 by fitting experimental data tested from cement pastes, and their comparisons also showed that the suggested value could lead to a larger resistance to vapor transport compared to soils, and the predicted results also agreed well with the actual observations in cementitious materials.

2.2 Multi-species Ionic Transport

In addition to the moisture transport, the governing equations for multi-ions transport process in unsaturated concrete, incorporating diffusion caused by concentration gradient, migration caused by multi-ions coupling effect, convection caused by moisture transport, and also ionic binding will be elaborated in this section. The mass conservation equation of individual ionic species in the concrete pore solution can be written as

$$\frac{\partial C_i}{\partial t} = -\nabla \cdot J_i \quad i = 1, ..., N \tag{10}$$

where C_i (mol/m^3) is the molar concentration of different ionic species in concrete pore solution; t (s) is the time; J_i (mol/m^2/s) is the ionic flux of the i-th ionic species, and N is the total number of the ionic species involved in the concrete pore solution. The ionic flux J_i of each ionic species can be expressed as follows:

$$J_i = -\underbrace{D_i \nabla C_i}_{\text{Diffusion}} - \underbrace{D_i C_i \left(z_i F / RT \right) \nabla \Phi}_{\text{Migration}} + \underbrace{u \cdot C_i}_{\text{Convection}} \tag{11}$$

where the three terms on the right side of Eq. (11) represent diffusion flux, migration flux, and convection flux, respectively; D_i (m²/s) is the diffusivity of each ionic species which can be determined by Eq. (18) in unsaturated condition; z_i is the charge number of each ionic species; F (94,680 C/mol) is the Faraday constant; R (8.314 J/mol/K) is the ideal gas constant; Φ (V) is the electrostatic potential. In order to determine the ionic convective flux due to the transport of bulk liquid water, the liquid water volume flux u (m/s) is introduced here, which can be determined through J_l/ρ_l.

Substituting Eq. (11) into Eq. (10), the governing equation for multi-ionic species transport characterizing the contribution from diffusion, migration and convection can be obtained as

$$\frac{\partial C_i}{\partial t} = \nabla \cdot \left[D_i \nabla C_i + D_i C_i \left(z_i F/RT \right) \nabla \Phi \right] - \nabla \cdot \left(u C_i \right) \tag{12}$$

During the ionic transport process, chloride ions can be chemically or physically fixed to cementitious materials, and this the so-called chloride binding phenomenon will also impact the chloride transport behavior in concrete (Li et al. 2019a, b). When free chloride ions penetrate into concrete, some chemically react with the hydration products to form Friedel's salt, and some are physically absorbed on the surface of the solid phase (Tang and Nilsson 1993). Therefore, the transport equation of chloride can be rewritten as

$$\frac{\partial C_{f,Cl}}{\partial t} + \frac{\partial C_{b,Cl}}{\partial t} = \nabla \cdot \left[D_{Cl} \nabla C_{Cl} + D_{Cl} C_{Cl} \left(z_{Cl} F/RT \right) \nabla \Phi \right] - \nabla \cdot \left(u C_{Cl} \right) \tag{13}$$

where $C_{b,Cl}$ (mol/m³) and $C_{f,Cl}$ (mol/m³) are the concentrations of bound chloride and free chloride, respectively. The relationship between free and bound chloride ions is known as chloride binding isotherm. In this study, the Langmuir binding isotherm has been adopted to depict the binding process which is described in Eq. (14).

$$C_{b,Cl} = \frac{a C_{f,Cl}}{w \left(1 + b C_{f,Cl} \right)} \tag{14}$$

where a and b are experimentally fitted constants; w is the weight ratio of evaporable water to concrete. Then, the chloride binding capacity λ can be used to represent the relations between the free and bound chloride concentration as follows.

$$\frac{\partial C_{b,Cl}}{\partial t} = \frac{\partial C_{b,Cl}}{\partial C_{f,Cl}} \cdot \frac{\partial C_{f,Cl}}{\partial t} = \lambda \cdot \frac{\partial C_{f,Cl}}{\partial t} \tag{15}$$

$$\lambda = \frac{a}{w \left(1 + b C_{f,Cl} \right)^2} \tag{16}$$

Therefore, substituting Eq. (15) and Eq. (16) into Eq. (13), the chloride binding isotherm can be integrated into transport equation of chloride ions, which can be expressed as

$$(1 + \lambda) \frac{\partial C_{f,Cl}}{\partial t} = \nabla \cdot \left[D_{Cl} \nabla C_{Cl} + D_{Cl} C_{Cl} \left(z_{Cl} F/RT \right) \nabla \Phi \right] - \nabla \cdot \left(u C_{Cl} \right) \tag{17}$$

Additionally, the influence of water diffusion on ionic diffusion coefficient in unsaturated condition should also be considered. According to the study by Saetta et al. (1993), the relative ionic diffusivities in unsaturated concrete can be expressed as a function of relative

Fig. 2 Normalized diffusion coefficient as a function of relative humidity
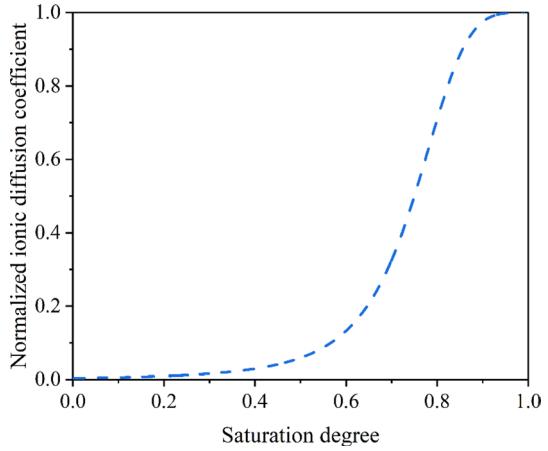
humidity in a S-shaped curve, which has been shown in Fig. 2 and can be consequently formulated as

$$D_i = D_{i,sat} / \left[1 + \left(\frac{1 - RH}{1 - RH_c} \right)^4 \right] \qquad (18)$$

where $D_{i,sat}$ represents the ionic diffusion coefficients in saturated concrete, RH_c represents relative humidity threshold suggesting that D_i is to half of its value at the fully saturated condition, and it was suggested to be taken as 0.75 by Saetta et al. (1993).

It should be noted here that, because of different diffusivities of various ionic species, the resulted concentration difference among the positive and negative charged ions will cause a charge imbalance ($\sum_{i=1}^{N} z_i C_i$, where i represents the label of ionic species) inside the concrete pore solution. The presence of the charge imbalance will further generate an electrostatic potential (Φ), which could affect the transport behavior of all the species of ions (Liu et al. 2012). This phenomenon is so called as the multi-ions coupling effect. Based on the electrochemical constitutive law, the electrostatic potential distribution caused by charge imbalance can be depicted by the Poisson equation as

$$\Delta \Phi = -\frac{F}{\varepsilon_0 \varepsilon_r} \sum_{i=1}^{N} z_i C_i \qquad (19)$$

where ε_0 (8.854×10^{-12} C/V/m) is the vacuum permittivity; ε_r (78.3) is the relative permittivity of water at the temperature of 293.15 K; N is the total number of ionic species in concrete pore solution. In this study, a total of four ionic species have been considered ($N=4$), so the ionic species labeled from 1 to 4 represent the sodium, potassium, chloride and hydroxyl ions, respectively.
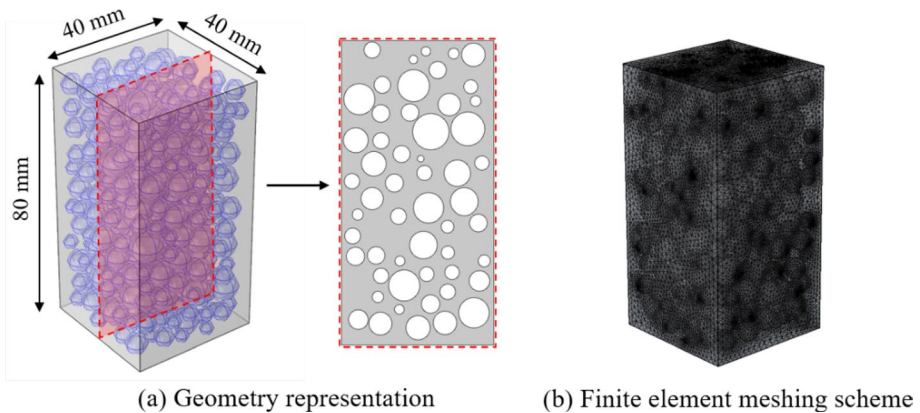
(a) Geometry representation   (b) Finite element meshing scheme

Fig. 3 Schematic diagram of (**a**) the geometrical representation in both 3D and 2D views and (**b**) finite element meshing scheme

3 Model Establishment

In this study, a three-dimensional model with the consideration of coarse aggregates instrument has been built, where coarse aggregates were randomly generated and packed in the matrix through an algorithm developed by the MATLAB platform. It should be noted that the size distribution of coarse aggregates was determined according to the Fuller grading curve, and the volume fraction of coarse aggregates can also get adjusted according to different concrete mix proportions. Here, a three-dimensional model sized 40 mm×40 mm×80 mm has been established, which is identical to the size of the prismatic specimens in the third-party experiment used for parameter calibration and model validation in Sect. 4. In terms of the geometric information of coarse aggregates, as an illustrative example, the maximum and minimum particle sizes have been set as 10 mm and 4 mm, respectively, and the volume fraction of coarse aggregates was set as 40%, as displayed in Fig. 3a. Besides, although coarse aggregates are irregular in real cases, they were represented as ideal spheres to reduce the mesh complexity and save computational cost in the presented numerical model.

After establishing the geometry part, a mesh sensitivity analysis has been conducted to determine the required element meshing size with a stable numerical solution. By continuously reducing mesh size until there is no obvious differences in the numerical results, a maximum element size of 1.5 mm has been determined, and the finite element meshing scheme is displayed in Fig. 3b. It should be noted that because of the low permeability of coarse aggregate, it has been treated as impermeable for both moisture and ions and was consequently not meshed in this study.

4 Parameters Calibration and Model Validation

The transport properties of concrete are dependent on various influence factors, so it is necessary to identify parameter values from experimental data to ensure the input parameters falling in a reasonable range. In this section, the key parameters related to the moisture and ionic transport will firstly be calibrated against the experimental results reported by Zhao
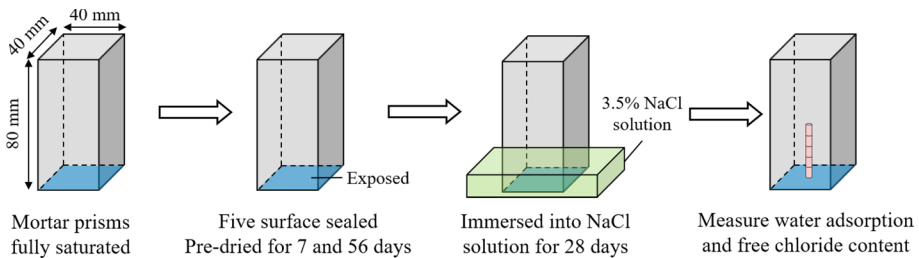
Fig. 4 Part of the experimental procedure conducted by Zhao et al. (2020)

et al. (2020). Then by keeping all calibrated parameters unchanged, the numerical results will then be compared with the experimental data obtained from the same experiment program which have not been used in the calibration stage to further testify the validity of the presented model. Part of the experimental procedure conducted by Zhao et al. is displayed by Fig. 4. Generally, two groups of prism specimens in fully saturated state were dried with only one surface exposed, where one group was dried for 7 days and the other for 56 days, respectively. Then, all specimens were immersed in 3.5% sodium chloride solution for 28 days to measure the water absorption capacity by weight difference method, and the free chloride content in concrete at the 7th day was also measured by grinding powder from the specimens. In addition, the sorption experiment was also conducted by Zhao et al. to determine the adsorption and desorption isotherms. It should be noted that coating surfaces would increase the air pressure in pores and block the mass transport. However, in the experiment by Zhao et al., the specimen was in a saturated state before pre-dried treatment. Therefore, air phases can only exist in the surface region, so the blocking effect may not be a dominant factor in the mass transport process.

In this study, the experiment data from group with 7-day drying were used for parameter calibration, and the experimental results from the group with 56-day drying stage were used for the model validation by keeping all previously calibrated parameters unchanged. Meanwhile, the boundary and initial conditions of ionic concentrations and saturation degree are set as identical to the experiment. It should be noted that the initial condition (i.e., water content profile) for the wetting period immersed in sodium chloride solution was calculated by modeling the previous drying process. In other words, the calculated water content profile from the drying process was used as the initial condition for the subsequent modeling of wetting. In addition, as for modeling of drying process, since Zhao et al. (2020) did not provide experimental data of the water content profiles after the predrying period, so only the results in wetting process were used for parameter calibration and model validation. However, the unknown water content profile after drying made the direct parameter calibration impossible. Therefore, the trial and error process was adopted to quantify the water permeability. In details, an approximate value for water permeability was preliminarily adopted in modeling the drying process, and the water content profiles were used as the initial condition of the subsequent wetting process. Then, the permeability was calibrated and adjusted according to the experimentally tested water adsorption results. Subsequently, the calibrated value was adopted to recalculate the entire drying and wetting process, and the calculated water adsorption content was compared with the experimental measurements. If the results do not match the experimental results well, this process will be continued until the relative error is acceptable.

Fig. 5 Sorption isotherms fitted through experimental data from Zhao et al. (2020)
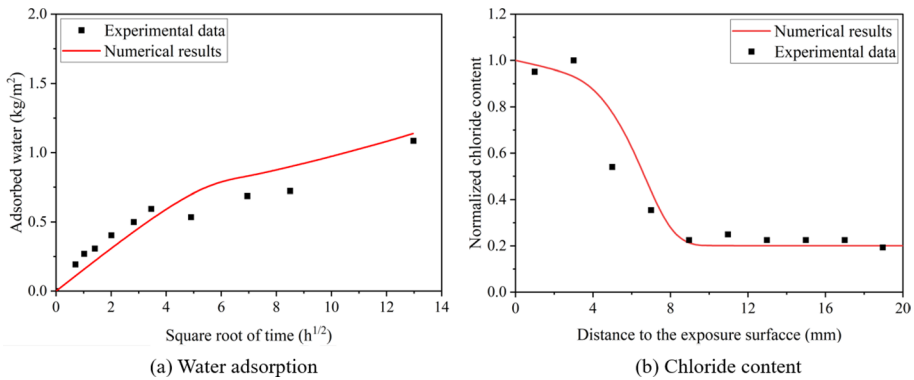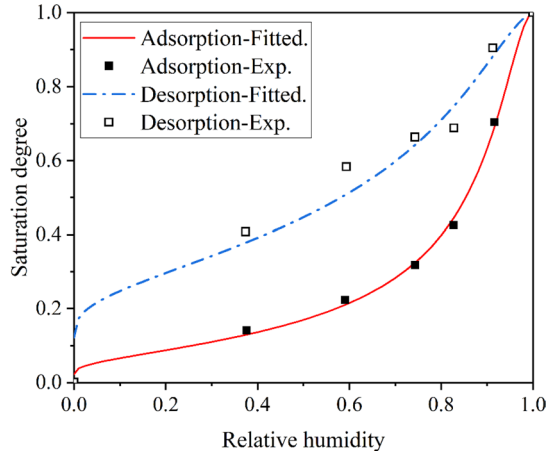

(a) Water adsorption

(b) Chloride content

Fig. 6 Parameter calibration against experiment results from Zhao et al.: (**a**) the amount of adsorbed water and (**b**) free chloride content

Firstly, according to the isothermal sorption experiment conducted in literature (Zhao, et al. 2020), the saturation degree was calculated by the mass difference during drying and wetting process, and the relative humidity was obtained by a humidity sensor. Subsequently, the sorption isotherms can be fitted according to the van Genuchten equation (i.e., Eq. (3)), as shown in Fig. 5. It can be observed that for both adsorption and desorption processes, the van Genuchten equation is capable of accurately fitting the sorption isotherms, and the fitting parameters α and m have been quantified as $\alpha = 1.026 \times 10^7$ Pa, $m = 0.444$ for adsorption, and $\alpha = 2.099 \times 10^7$ Pa, $m = 0.340$ for desorption, respectively.

As for the moisture transport, the liquid water permeability in concrete should be calibrated against the experimental results. According to the capillary imbibition test results measured by Zhao et al. (2020) (i.e., the amount of water adsorption versus imbibition time), the parameter used to depict the decayed water permeability in Eq. (6) can be quantified as: $K_0 = 21.4 \times 10^{-21}$ m^2, $K_1 = 0.21 \times 10^{-21}$ m^2, $\gamma = 0.8$, and $\tau = 3600$ s, as shown in Fig. 6a. The calibration process adopted the trial and error procedure to reduce the differences between numerical results and experimental measurements, where various sets of parameters have been tested and the group with optimal numerical results were selected.

Table 1 Quantified parameters in the present numerical model

Parameters	Symbols	Values	Data sources
Permeability	K_0	21.4×10^{-21} m^2	(Zhao et al. 2020)
Permeability	K_1	0.12×10^{-21} m^2	(Zhao et al. 2020)
Exponent	γ	0.8	(Zhao et al. 2020)
Decay time	τ	3600 s	(Zhao et al. 2020)
Diffusivity of vapor in air	D_v^0	2.45×10^{-5} m^2/s	(Li and Li 2013)
Adsorption isotherm fitting parameters	α and m	1.026×10^7 Pa, 0.444	(Zhao et al. 2020)
Desorption isotherm fitting parameters	α and m	2.099×10^7 Pa, 0.340	(Zhao et al. 2020)
Chloride diffusion coefficient	$D_{Cl,sat}$	8.52×10^{-12} m^2/s	(Zhao et al. 2020)
Sodium diffusion coefficient	$D_{Na,sat}$	5.59×10^{-12} m^2/s	Normalized
Potassium diffusion coefficient	$D_{K,sat}$	8.21×10^{-12} m^2/s	Normalized
Hydroxyl diffusion coefficient	$D_{OH,sat}$	2.20×10^{-11} m^2/s	Normalized

By taking into the time dependence nature of water permeability, it can be seen that the imbibed water content showed an obvious deviation from the square root of time law.

Besides, in terms of the chloride diffusion coefficients, according to the experimentally tested free chloride concentrations by drilling powders from the specific depths of the specimens, the chloride diffusion coefficient in saturated condition has been calibrated as $D_{Cl,sat} = 8.52 \times 10^{-12}$ m^2/s following a trial and error process, as illustrated in Fig. 6b. Although the calibrated diffusion coefficient was in the general range of values, relative errors still existed between the numerical result and experiment measurements of the free chloride concentrations. The differences may be introduced by the test error from the experiment, and the chloride binding process was not explicitly expressed in the numerical model, which can also cause chloride concentration differences in the penetration depth from 4 to 8 mm. However, considering the fact that no bound chloride concentrations have been provided in the aforementioned experimental study, it is difficult to quantify the exact value of chloride binding parameters. Based on the classic chloride binding experiment by Tang et al. (1993), where the binding capacity of OPC mortars with a water-to-cement ratio of 0.4 were tested (identical to the experiment used for calibration), the fitting parameters for Langmuir isotherms are adapted as $a = 0.417$ and $b = 0.077$. Note that the precise values for chloride binding parameters are still required to further improve the model accuracy.

As for the diffusion coefficient of other ionic species such as sodium and potassium ions, considering the difficulties of directly measuring their diffusion coefficients, their values can be determined based on the normalized value between calibrated chloride diffusion coefficient and its diffusion coefficient in water solution. However, it should be noted that the exact values of diffusion coefficients would vary between different cementitious materials systems, and normalizing from the values in bulk water was a bit rough method to generally satisfy the need of calculating the charge imbalance, and more sophisticated methods should be employed in the future study. Besides, the ionic diffusion coefficient in unsaturated condition can be subsequently determined by Eq. (18) depending on the relative humidity. For now, parameters adopted in the numerical model have been determined, and their values are listed in Table 1. The corresponding data sources have also been provided in Table 1. However, it should be noted that although the parameters listed in Table 1 are calibrated, directly selected or normalized from different data sources, which may limit the model applicability, the materials form
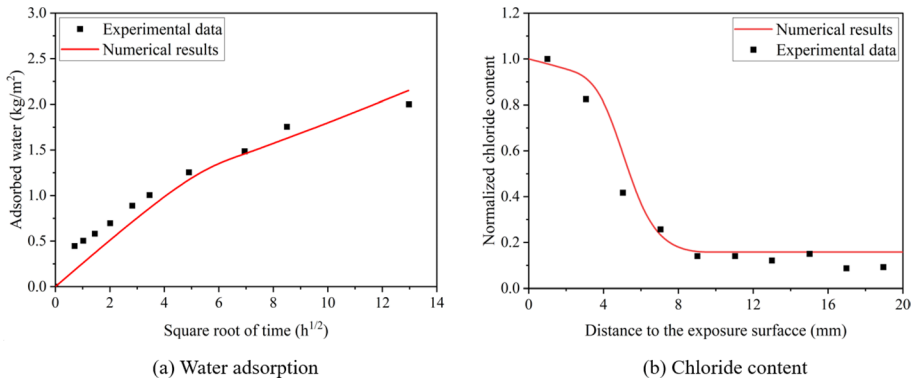
(a) Water adsorption

(b) Chloride content

Fig. 7 Results comparison between numerical model and experimental measurement on (**a**) water adsorption and (**b**) free chloride content

Table 2 Initial and boundary concentrations of ionic species in the model

Ionic species	Initial concentration (mol/m^3)	Boundary concentration (mol/m^3)
Cl$^-$	0	590
Na$^+$	285	590
OH$^-$	385	0
K$^+$	100	0

the mentioned data sources are all ordinary Portland cement concrete. However, it is still recommended to use the experimentally measured parameters or calculations from more sophisticated methods when applying this model in another situation.

Without changing the above calibrated parameters, the specimen group with 56-day drying have been modeled and the numerical results were then compared to the experimental measurements. The numerical and experimental results on the amount of water adsorption and chloride concentration are compared in Fig. 7a, b, respectively. It can be observed that the amount of adsorbed water possesses an almost linear relationship with the square root of exposure time, and this phenomenon can also get well reflected by the numerical modeling results. As for the chloride concentration distribution after 56-day exposure to the 3.5% sodium chloride solution, it can be found that the chloride concentration gradually reduces along the penetration depth, and the numerical results coincide well with the experimental data, which can also testify the validity of the model from the perspective of ionic transport.

5 Results and Discussion

In order to better understand the potential influence factors of the coupled moisture and multi-ionic transport in unsaturated concrete, a detailed parametric analysis will be conducted in this section. In this section, the model geometry information was identical to that mentioned in Sect. 3. The model has been set as only the bottom surface exposed to the 3.5% sodium chloride solution (approximately 590 mol/m^3 in molar concentration), and
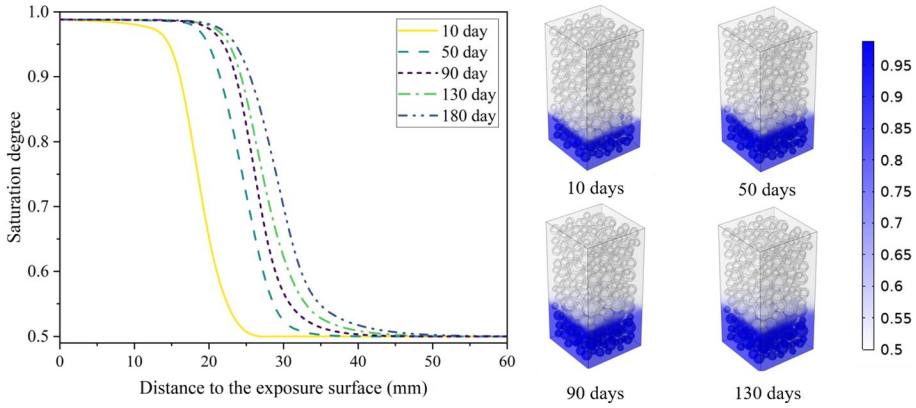
Fig. 8 Distribution of moisture saturation at different exposure time

(a) Chloride concentration after 10 days

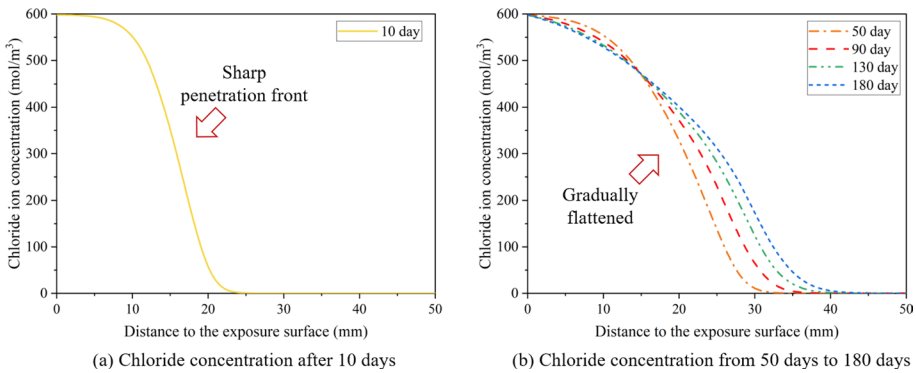(b) Chloride concentration from 50 days to 180 days

Fig. 9 Chloride concentration distributions (**a**) from 20 to 80 days before concrete saturated and (**b**) from 80 to 160 days after concrete saturated

the initial ionic concentrations in concrete pore solution are listed in Table 2. The initial saturation degree was firstly set as 50% unless otherwise mentioned in the parametric analysis. After an overview of the general results of moisture and multi-ionic transport, the multi-ions coupling effect, especially under the unsaturated condition, will be compared to the electro-neutrality assumption, and the influence of electrostatic potential induced by charge imbalance on multi-ionic transport behaviors is analyzed. Then, the influence of initial saturation degree on moisture transport and ionic concentration will also be discussed. In addition, the effect of concrete heterogeneity and modeling dimensions on the prediction results have also been studied.

5.1 Overview

The distributions of saturation degree at various exposure time are shown in Fig. 8. It can be seen from the figure that although the wetting front moves deeper in concrete and the inner capillary pores tend to get saturated with time, adsorption rate gradually reduces because of the decayed water permeability. After 10 days, the wetting front has reached
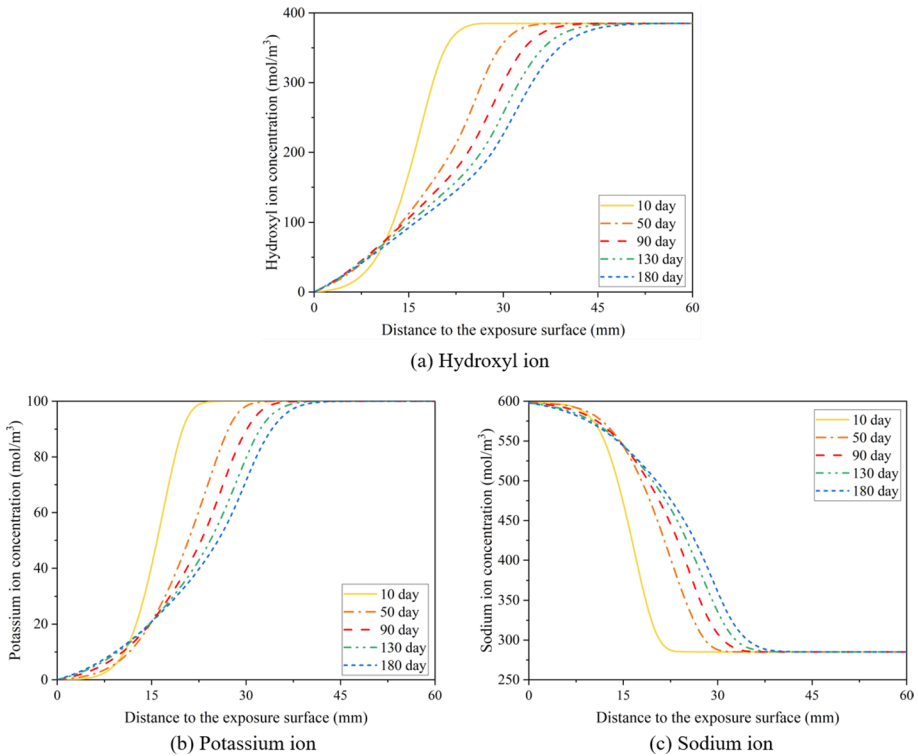
Fig. 10 Ionic concentration distributions of (**a**) hydroxyl ions, (**b**) potassium ions and (**c**) sodium ions

25 mm. It can be noticed that the moisture transport rate gradually reduces as the wetting front moves deeper into the concrete, and the wetting front can maximumly reach 50 mm after 180-day exposure. In addition, it can be also found that because of the intrusion of coarse aggregates, the distribution of saturation degree is not uniform inside the concrete, which is mainly caused by the blocking effect of coarse aggregates on mass transport.

The free chloride concentration profiles after 10-day exposure (i.e., during the rapid moisture adsorption period) and that from 50 to 180 days have been displayed in Fig. 9a, b, respectively. It can be found that the chloride concentration distributions are influenced by the moisture adsorption rate and also the water permeability. As illustrated in Fig. 9a, the sharp penetration front can be noticed after 10-day exposure when the capillary imbibition is still significant as shown in Fig. 8. This is because during the transport process of moisture, free chloride ions dissolved in water will also enter the concrete. Because the moisture transport is much faster than the chloride ion diffusion, the chloride transport is mainly dominated by the convection before saturation. On the contrary, when the water permeability has decayed to a lower value, that is from 50 days in this study, the chloride transport process is dominated by diffusion, as illustrated in Fig. 9b. In addition to the gradually flattened concentration gradient, it can be found that the chloride concentration in the area with penetration depth smaller than 15 mm is even decreasing with time. This is because the concentration gradient in the area with concrete cover thickness less than 10 mm was smaller than that between 15 and 30 mm.
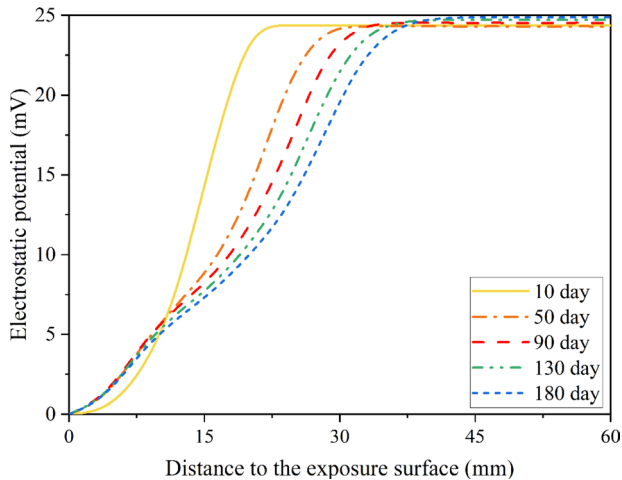
Fig. 11 Electrostatic potential distribution at different exposure time

With the extension of exposure, chloride ions supplied from the concrete area within 10 mm are less than those diffused inward. As a result, the chloride ion concentration between 40 and 60 mm is reducing with time, and the chloride ions concentration deeper than 60 mm is increasing, which makes the concentration front more flatten.

The concentration distributions of other ionic species including hydroxyl ions, sodium ions and potassium ions have been shown in Fig. 10. It can be seen, similarly to the chloride, the transport behaviors of these ionic species are also firstly controlled by convection at the initial stage, and then by diffusion with the gradually decayed water permeability. In addition, the sharp concentration gradient formed at the convection controlled stage also gradually becomes flattened during the diffusion controlled stage, which is similar to that observed from the chloride concentration profiles.

5.2 Effect of Electrostatic Potential Caused by Multi-ions Coupling

Because of the different diffusivities and carried charges of different ionic species, a charge imbalance will be caused in concrete pore solution during the ionic transport process, and an electrostatic potential inside the concrete will be consequently introduced to further influence the ionic transport behavior, which has been called as the multi-ions coupling effect. In order to characterize the electrical coupling among different species, the presented work adopts the Poisson equation, as given by Eq. (19), to determine the evolvement of electrostatic potential during the ionic transport in unsaturated condition.

The evolution of electrostatic potential at the different exposure time is shown in Fig. 11. Even though no external voltage or current is applied, the maximum electrostatic potential approximates 25 mV. Meanwhile, it can be found from the figure that the distribution of electrostatic potential is space- and time dependent due to the variation of ionic concentration and charge imbalance inside concrete pore network. However, with the increase of exposure time, the amplitude of electrostatic potential gradually decreases, which agrees well with the phenomenon observed by Johannesson et al. (2009). This can be explained by the fact that as time goes by, the ionic species in concrete tends to be in an equilibrium state, and the charge imbalance introduced by external ionic penetration would gradually
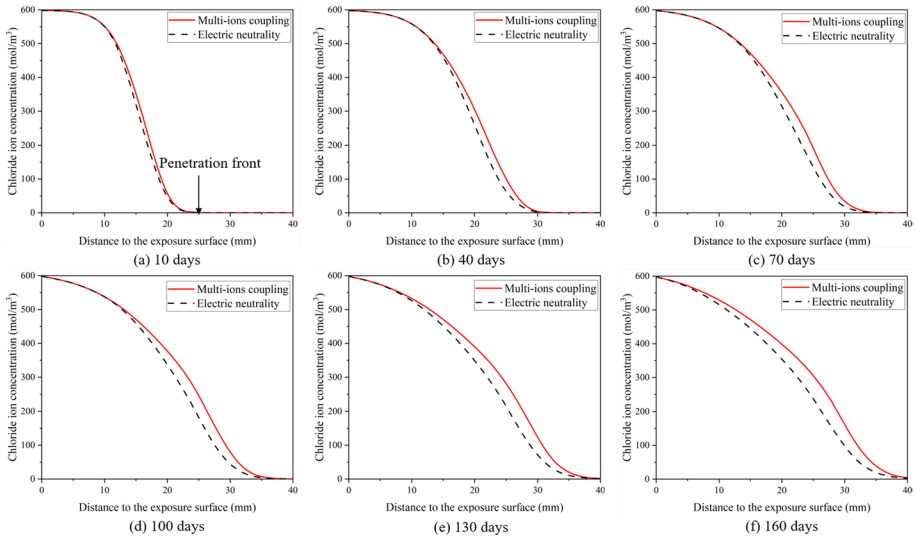
Fig. 12 Comparisons of chloride ion concentrations calculated by considering multi-ions coupling effect and electro-neutrality assumption

become less significant, which has led to the reduced electrostatic potential. In addition, it can also be found that the position of the maximum electrostatic potential often appears in a deeper position with the extension of exposure time. This is because the severest charge imbalance takes place where the ionic transport wavefront has reached. As a result, the more obvious electrostatic potential tends to appear at the penetration front.

In addition, Samson and Marchand (2007) developed a multi-species transport model in unsaturated concrete with the consideration of chemical equilibriums, and the calculation of the model was based on the operator splitting approach. Although the moisture transport was not modeled in this reactive transport model, their results still highlighted that implementation of the chemical equilibriums in the transport modeling can successfully reproduce the chemical effect of the precipitation and dissolution, and the influence of electrochemical coupling can also result in a more accurate prediction against the experimental data. Subsequently, Glasser et al. (2008) developed a comprehensive numerical model which includes the transport of ions, moisture and gas, and they reported that the moisture content in concrete has a significant influence on chloride transport behavior, which is consistent with the results from this study. Besides, due to the advantages of taking moisture into account, the numerical model developed by Glasser et al. was capable of simulating various durability degradation processes such as steel corrosion and carbonation which have a closer relationship with moisture content.

In order to further illustrate the influence of electrostatic potential on ionic transport behavior, the chloride concentrations calculated with and without the consideration of multi-ions coupling effect have been compared in Fig. 12. It can be observed that because of the positive electrostatic potential introduced by the multi-ions coupling effect, the penetration of chloride ions as anions can be accelerated, which will eventually lead to a higher chloride content when the multi-ions coupling effect has been considered. However, for electro-neutrality assumption, since there is no contribution from the ionic migration, the chloride content is lower than that calculated by taking multi-ions coupling effect into

Fig. 13 Averaged chloride concentration after 180 days with and without the consideration of multi-ions coupling effect
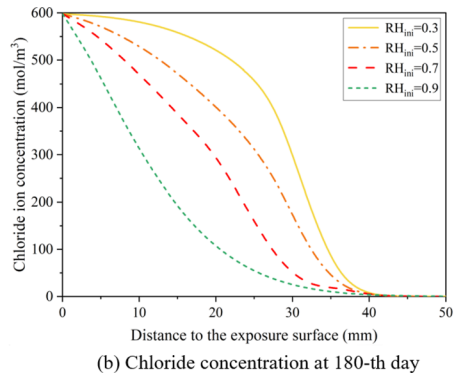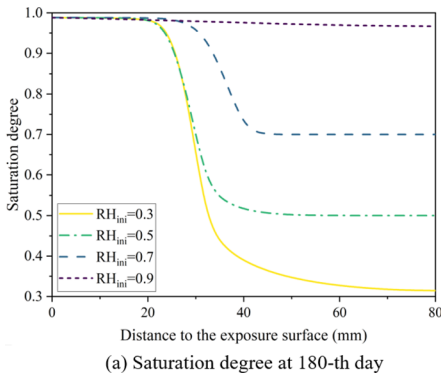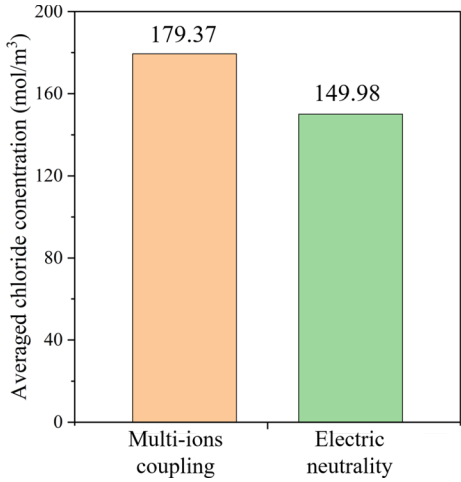

Fig. 14 The distribution of (**a**) saturation degree after 20 days and (**b**) chloride concentration after 180 days with various initial moisture content

(a) Saturation degree at 180-th day

(b) Chloride concentration at 180-th day

account, which suggests that the electro-neutrality assumption will underestimate the chloride concentration. In addition, it can also be noticed from the figure that the influence of multi-ions coupling effect is much more obvious at the depth lower than the penetration front. This is attributed to the fact that the charge imbalance is most serious at the penetration front where the induced electrostatic potential is larger as shown in Fig. 11. Therefore, with the increase in exposure time and gradual moving inward of the chloride penetration front, the concentration difference at the position where the penetration front has passed is more significant.

Although the contribution of multi-ions coupling effect was not obvious enough before 40-day exposure, a significant difference in chloride concentration can be noticed from the 100-th day, as can be observed from Fig. 12d–f. Besides, Figure 13 displays the averaged free chloride concentration calculated by models with and without considering the multi-ions coupling effect. It is shown that after 180-day exposure, the averaged chloride concentration can be underestimated by 1.2 times lower when adopting the electric neutrality

Fig. 15 The influence of initial saturation on electrostatic potential distribution after 180-day exposure
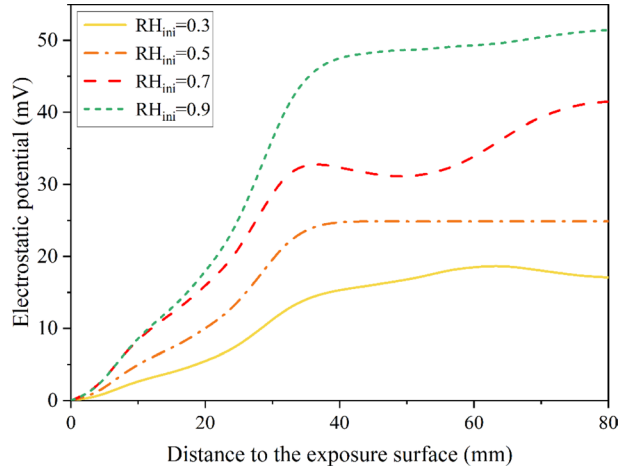
assumption in unsaturated concrete. It therefore again highlights the importance of considering multi-ions coupling effect in predicting the chloride penetration.

5.3 Effect of Initial Saturation

Figure 14 illustrates the influence of initial saturation degree on the distribution of moisture content after and chloride concentration after 180-day exposure, respectively, where the initial saturation degree has been set as 0.3, 0.5, 0.7 and 0.9. It can be seen from Fig. 14a that lower initial saturation degree leads to a larger capillary adsorption rate. As for the chloride concentration, it can be can found from Fig. 14b that the smaller initial saturation degree will enlarge the effect of convection, which eventually leads to a higher chloride concentration in concrete pore solution. This indicates that compared to the fully saturated concrete, partially saturated concrete is more vulnerable to chloride attack due to the convection effect. In addition, the initial saturation degree also influences the chloride concentration distribution pattern. For concrete with lower initial saturation degree, the transport is mainly convection controlled where a sharp penetration front can be found. However, for concrete with larger saturation degree such as 90%, the chloride concentration distribution profile is a gentle curve and no sharp penetration front is observed.

In addition to the moisture and ionic transport, the effect of initial saturation on electrostatic potential evolvement is shown in Fig. 15. It can be observed from the figure that lower initial saturation degree will lead to a smaller electrostatic potential, and the electrostatic potential of concrete with 30% initial saturation is lower than that of concrete with 90% initial saturation. This phenomenon can be mainly explained from the following two aspects. On the one hand, lower initial moisture content will enlarge the convection effect, which will facilitate the ionic transport in concrete pore network. Because the charge imbalance will gradually reduce with the continuous ionic transport, the charge imbalance caused by external ionic penetration will turn back to the balance state much more quickly with the increased ionic transport speed. On the other hand, with a larger initial saturation, ionic species are provided with more space in the pore solution to interact with other species leading to a more significant charge imbalance, which would also enlarge
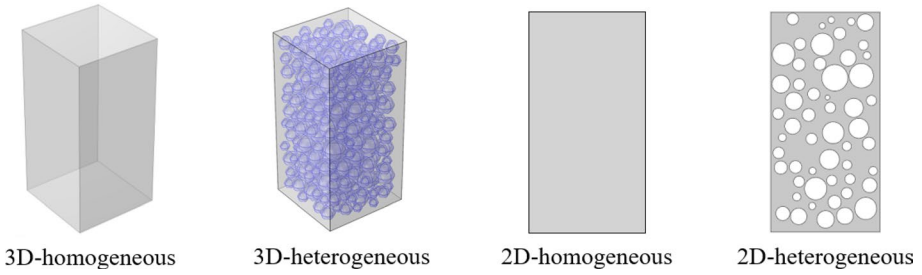
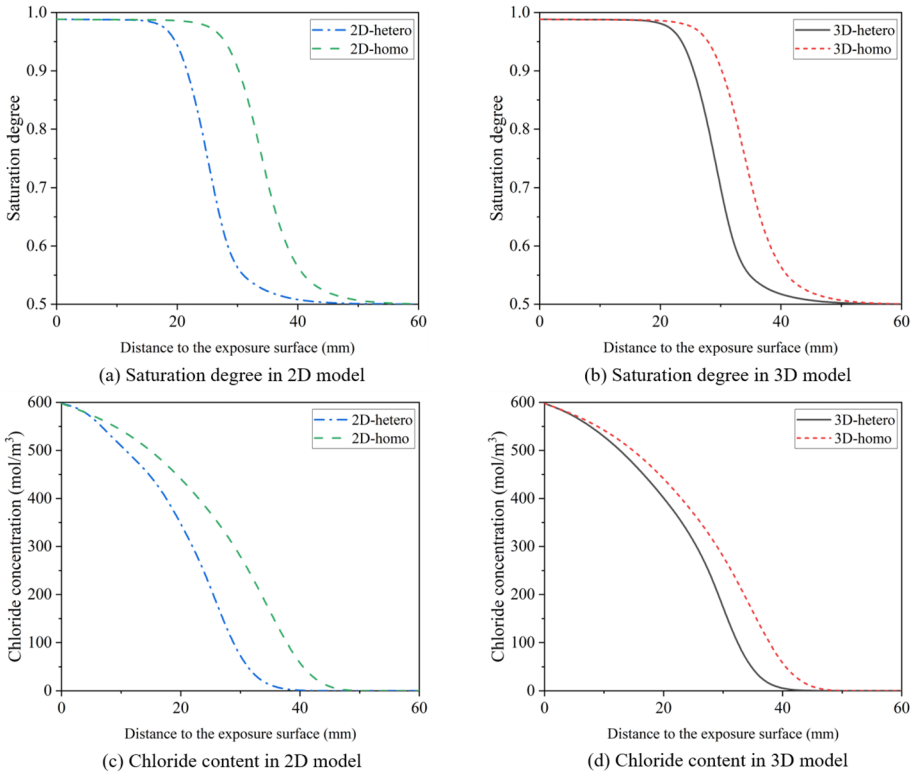**Fig. 16** Four models with different dimensions and heterogeneities

Fig. 17 The influence of concrete heterogeneity on moisture and chloride content for both 2D and 3D cases

the electrostatic potential. Therefore, the charge imbalance is less obvious for less saturated concrete, and the electrostatic potential caused by the charge imbalance is also less significant.
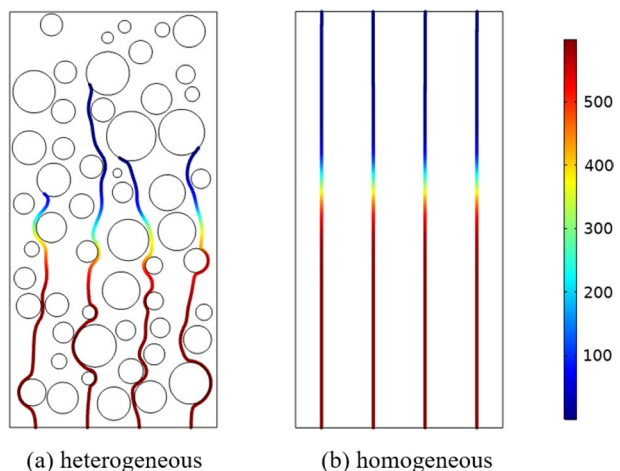
5.4 Effect of Heterogeneous Nature

In order to further illustrate the impact of concrete heterogeneous nature on mass transport, the influence of coarse aggregates existence will be discussed. In this section, a total of four models with have been built including 3D homogeneous model, 3D heterogeneous model, 2D homogenous model and 2D heterogeneous model, as shown in Fig. 16. It should be noted that the geometry of 2D heterogeneous model is selected from the longitudinal section of 3D heterogeneous one, and only the bottom surface (or side in two-dimensional cases) has been set as exposed to the external solution.

The saturation degree and chloride concentration calculated by homogenous and heterogeneous models in both two-dimensional and three-dimensional cases are compared in Fig. 17. It can be found that although more obvious for two-dimensional cases, both the saturation degree and chloride concentration calculated by heterogeneous models are smaller than the homogeneous models. This is mainly because the heterogeneity caused by coarse aggregates instrument will introduce a blocking effect on mass transport. In other words, because of the low permeability of aggregates, ions and moisture can hardly transport through aggregates but can only move around them, as shown by the steam line in Fig. 18, which extends the mass transport path and leads to a reduced moisture and ionic transport rate.

5.5 Effect of Modeling Dimensions

It should be noted that most of the existing models focusing on the coupled ionic and moisture transport were built in one-dimension or two-dimension, which leads certain differences with the mass transport in real cases. Therefore, it is necessary to investigate the influence of modeling dimensions on the results of mass transport. As shown in Fig. 19, the saturation degree and chloride concentration distribution calculated by three-dimensional model and two-dimensional model have been compared. It can be found that for heterogeneous models which have taken the influence of coarse aggregates into account, both the saturation degree and chloride concentration calculated by 2D model were smaller than in 3D case. The maximum difference can reach 1.40 and 3.52 times for saturation

Fig. 18 The stream lines of chloride ions for the (**a**) heterogeneous case and (**b**) homogeneous case

(a) heterogeneous   (b) homogeneous

(a) Saturation degree in heterogeneous model

(b) Saturation degree in homogeneous model

(c) Chloride content in heterogeneous model
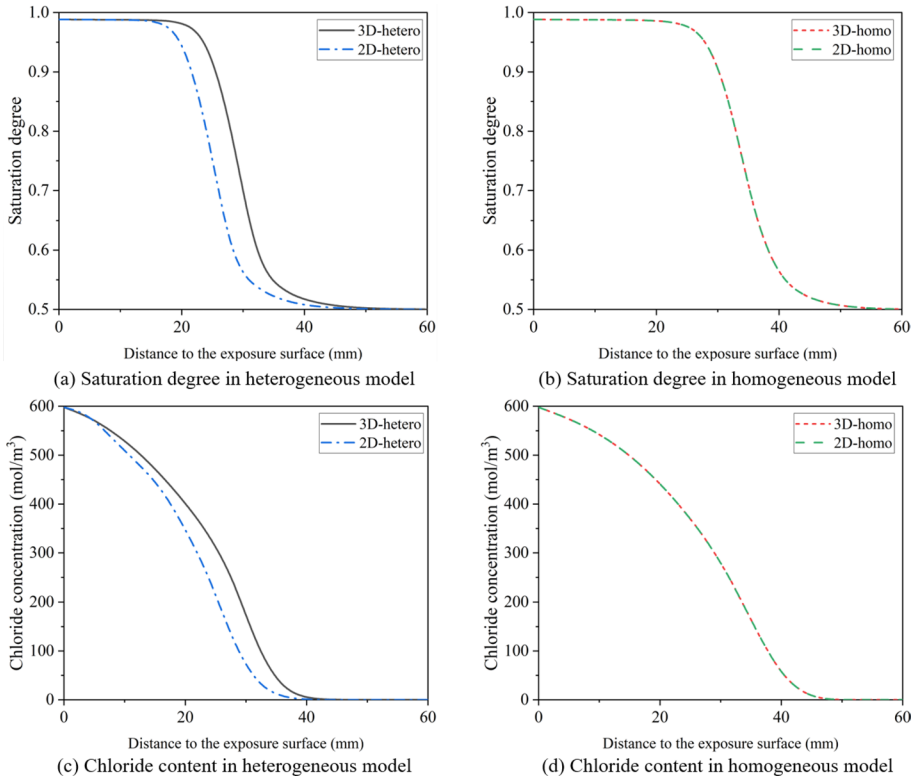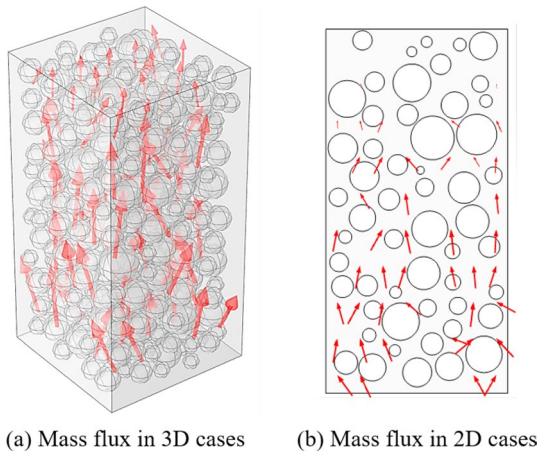
(d) Chloride content in homogeneous model

Fig. 19 The influence of modeling dimensions on moisture and chloride content for both heterogeneous and homogeneous cases

Fig. 20 Schematic diagram of the mass flux pattern in 3D and 2D cases

(a) Mass flux in 3D cases (b) Mass flux in 2D cases

degree and chloride concentration, respectively. This can be explained by the fact that the mass flux on the third direction cannot get well reflected in two-dimensional plane models. However, as for three-dimensional models, the mass flux around coarse aggregates can

also contribute to the moisture and chloride transport, which can to some extent contribute to the mass transport in porous media, as illustrated in Fig. 20. In addition, it can also be observed from Fig. 19b, d that when building model with the homogeneous assumption, the modeling dimension has little impact on the calculation results. This is because without the intrusion of coarse aggregates, the stream line of mass flux will follow almost straight lines in both 3D, 2D and even 1D cases, so the impact modeling dimension is negligible.

5.6 Current Limitations and Future Prospects

In this study, influence factors such as multi-ions coupling effect, initial saturate degree and modeling dimensions and heterogeneity have been discussed, but limitations still exist in the presented numerical model and future work could address the following aspects for further improvement.

- For porous material such as concrete exposed to saline environment, the dissolution of ionic species in pore solution will alter water activity and impact the chemical equilibrium relationships. Therefore, the influence of chemical speciation should be considered to more accurately depict the interactions among water transport, multi-ionic transport and chemical reactions.
- The chloride binding phenomenon was considered by Langmuir binding isotherm in this study. However, more accurate and comprehensive characterization of chloride binding can be modeled by taking chemical equilibriums into account. Other chemical reactions between ionic species and hydrated cement system can also the included to more realistically reflect the reactive transport behaviors.
- The transport properties in microscale and the influence of pore structure evolution can be considered to more comprehensively reveal the transport behavior in unsaturated concrete. Therefore, the existence of interfacial transitional zone and the anomalous transport phenomenon induced by different transport properties between large and small pores need to be essentially studied in the future studies.
- As for the input transport parameters, the presented model determined them by calibration or selecting from previous studies. However, since the transport properties may vary with different mixture proportions, and rough estimation of the transport property parameters would make the numerical results less quantitatively valuable, more accurate determination procedure such as experimental measurement and fitting with more sufficient data should be considered.

6 Conclusions

This work established a numerical model to investigate the moisture and multi-species ionic transport in unsaturated concrete. The moisture transport in concrete has been considered as two phases including both water vapor and liquid, and the anomalous moisture transport phenomenon has also been explicitly considered to better mimic the water transport in cementitious materials. The electrostatic potential induced by charge imbalance in concrete pore solution was solved by the Poisson equation to better understand the impact of multi-ions coupling effect on ionic transport especially under unsaturated condition. Key parameters adopted in the presented model has been calibrated, and the numerical results

have also been compared to experimental data to validate the presented numerical model. Then a parametric analysis has been conducted to investigate potential influence factors on the moisture and multi-ionic transport in unsaturated concrete. The major conclusions drawn from the study can be summarized as follows.

- The influence of water imbibition on the distribution pattern and magnitude of electrostatic potential is firstly investigated. For a single wetting process, although the magnitude of electrostatic potential at the same depth reduces, the distribution pattern is found to be not only related to ionic penetration but also to the water imbibition front, which is distinctively different to that observed in saturated transport condition.
- The positive electrostatic potential will still facilitate the penetration process of anions such as chloride. After 180-day exposure, the averaged chloride concentration can be underestimated by 1.2 times lower when adopting the electric neutrality assumption in unsaturated concrete.
- The initial saturation degree has an impact on both ionic transport and multi-ionic coupling intensity. In addition to improving the convection intensity under low saturate degree, higher initial saturation degree can also amplify the electrostatic coupling effect and level the amplitude up to 50 mV with a 90% initial saturation degree.
- The influence of modeling dimension and the model heterogeneity should be considered simultaneously. When considering the heterogeneity nature of concrete under two dimensions, the model cannot reflect the heterogeneity and mass flow in the third direction, which can result in 1.40 and 3.52 times lower prediction values for moisture and chloride content, respectively.

Declarations

Conflict of interest The authors declare that they have no competing interests and personal relationships that could influence the work in this paper.

References

Bao, J.W., Li, S.G., Zhang, P., Ding, X.Y., Xue, S.B., Cui, Y.F., Zhao, T.J.: Influence of the incorporation of recycled coarse aggregate on water absorption and chloride penetration into concrete. Constr. Build. Mater. **239**, 117845 (2020)

Baroghel-Bouny, V., Thiery, M., Wang, X.: Modelling of isothermal coupled moisture-ion transport in cementitious materials. Cem. Concr. Res. **41**(8), 828–841 (2011)

Bažant, Z.P., Najjar, L.J.: Nonlinear water diffusion in nonsaturated concrete. Matériaux Constr. **5**(1), 3–20 (1972)

Bertolini, L., Redaelli, E.: Throwing power of cathodic prevention applied by means of sacrificial anodes to partially submerged marine reinforced concrete piles: results of numerical simulations. Corros. Sci. **51**(9), 2218–2230 (2009)

Cai, Y., Liu, Q.F.: Stability of fresh concrete and its effect on late-age durability of reinforced concrete: An overview. J. Build. Eng. 179, 107701 (2023)

Caggiano, A., Schicchi, D.S., Mankel, C., Ukrainczyk, N., Koenders, E.A.B.: A mesoscale approach for modeling capillary water absorption and transport phenomena in cementitious materials. Comput. Struct. **200**, 1–10 (2018)

Cerny, R., Pavlik, Z., Rovnanikova, P.: Experimental analysis of coupled water and chloride transport in cement mortar. Cem. Concr. Compos. **26**(6), 705–715 (2004)

Chen, W., Liu, Q.: Moisture and multi-ions transport in concrete under drying-wetting cycles: a numerical study. J. Hydraul. Eng. **52**(5), 622–632 (2021)

Climent, M.A., de Vera, G., Lopez, J.F., Viqueira, E., Andrade, C.: A Test method for measuring chloride diffusion coefficients through nonsaturated concrete-part I the instantaneous plane source diffusion case. Cem. Concr. Res. **32**(7), 1113–1123 (2002)

de Vera, G., Climent, M.A., Viqueira, E., Anton, C., Andrade, C.: A test method for measuring chloride diffusion coefficients through partially saturated concrete part II: the instantaneous plane source diffusion case with chloride binding consideration. Cem. Concr. Res. **37**(5), 714–724 (2007)

Elakneswaran, Y., Iwasa, A., Nawa, T., Sato, T., Kurumisawa, K.: Ion-cement hydrate interactions govern multi-ionic transport model for cementitious materials. Cem. Concr. Res. **40**(12), 1756–1765 (2010)

Frizon, F., Lorente, S., Ollivier, J.P., Thouvenot, P.: Transport model for the nuclear decontamination of cementitious materials. Comput. Mater. Sci. **27**(4), 507–516 (2003)

Fu, C.Q., Ye, H.L., Jin, X.Y., Jin, N.G., Peng, Z.X.: Chloride penetration into concrete damaged by uniaxial tensile fatigue loading. Constr. Build. Mater. **125**, 714–723 (2016)

Garbalinska, H., Kowalski, S.J., Staszak, M.: Moisture transfer between unsaturated cement mortar and ambient air. Transp. Porous Med. **85**(1), 79–96 (2010)

Glasser, F.P., Marchand, J., Samson, E.: Durability of concrete-degradation phenomena involving detrimental chemical reactions. Cem. Concr. Res. **38**(2), 226–246 (2008)

Guimaraes, A.T.C., Climent, M.A., de Vera, G., Vicente, F.J., Rodrigues, F.T., Andrade, C.: Determination of chloride diffusivity through partially saturated Portland cement concrete by a simplified procedure. Constr. Build. Mater. **25**(2), 785–790 (2011)

Hall, C.: Water sorptivity of mortars and concretes—a review. Mag. Concr. Res. **41**(147), 51–61 (1989)

Hall, C.: Capillary imbibition in cement-based materials with time-dependent permeability. Cem. Concr. Res. **124**, 105835 (2019)

Homan, L., Ababneh, A.N., Xi, Y.P.: The effect of moisture transport on chloride penetration in concrete. Constr. Build. Mater. **125**, 1189–1195 (2016)

Hosokawa, Y., Yamada, K., Johannesson, B., Nilsson, L.O.: Development of a multi-species mass transport model for concrete with account to thermodynamic phase equilibriums. Mater. Struct. **44**(9), 1577–1592 (2011)

Hosokawa, Y., Yamada, K., Takahashi, H.: Time dependency of Cl diffusion coefficients in concretes with varied phase compositions and pore structures under different environmental conditions. J. Adv. Concr. Technol. **10**(11), 363–374 (2012)

Hou, D.S., Yu, J., Wang, P.: Molecular dynamics modeling of the structure dynamics, energetics and mechanical properties of cement-polymer nanocomposite. Compos. Part B Eng. **162**, 433–444 (2019)

Jensen, M.M., Johannesson, B., Geiker, M.R.: A numerical comparison of ionic multi-species diffusion with and without sorption hysteresis for cement-based materials. Transp. Porous Med. **107**(1), 27–47 (2015)

Johannesson, B.F.: A theoretical model describing diffusion of a mixture of different types of ions in pore solution of concrete coupled to moisture transport. Cem. Concr. Res. **33**(4), 481–488 (2003)

Johannesson, B.: Comparison between the Gauss' law method and the zero current method to calculate multi-species ionic diffusion in saturated uncharged porous materials. Comput. Geotech. **37**(5), 667–677 (2010a)

Johannesson, B.: Development of a generalized version of the Poisson-Nernst-Planck equations using the hybrid mixture theory: presentation of 2d numerical examples. Transp. Porous Med. **85**(2), 565–592 (2010b)

Johannesson, B., Yamada, K., Nilsson, L.O., Hosokawa, Y.: Multi-species ionic diffusion in concrete with account to interaction between ions in the pore solution and the cement hydrates. Mater. Struct. **40**(7), 651–665 (2007)

Johannesson, B., Hosokawa, Y., Yamada, K.: Numerical calculations of the effect of moisture content and moisture flow on ionic multi-species diffusion in the pore solution of porous materials. Comput. Struct. **87**(1–2), 39–46 (2009)

Khitab, A., Anwar, W., Arshad, M.T.: Predictive models of chloride penetration in concrete: an overview. J. Eng. Appl. Sci. **1**(1), 1–14 (2017)

Li, K.F., Li, C.Q.: Modeling hydroionic transport in cement-based porous materials under drying-wetting actions. J. Appl. Mech. Trans. Asme **80**(2), 020904 (2013)

Li, L.Y., Page, C.L.: Finite element modelling of chloride removal from concrete by an electrochemical method. Corros. Sci. **42**(12), 2145–2165 (2000)

Li, D.W., Wang, X.F., Li, L.Y.: An analytical solution for chloride diffusion in concrete with considering binding effect. Ocean Eng. **191**, 106549 (2019a)

Li, D.W., Li, L.Y., Wang, X.F.: Chloride diffusion model for concrete in marine environment with considering binding effect. Mar. Struct. **66**, 44–51(2019b)

Liu, Q.: Multi-phase modelling of concrete at meso-micro scale based on multi-species transport. J. Chin. Ceram. Soc. **46**(8), 1074–1080 (2018)

Liu, Q.F., Li, L.Y., Easterbrook, D., Yang, J.: Multi-phase modelling of ionic transport in concrete when subjected to an externally applied electric field. Eng. Struct. **42**, 201–213 (2012)

Liu, Q.F., Easterbrook, D., Yang, J., Li, L.Y.: A three-phase, multi-component ionic transport model for simulation of chloride penetration in concrete. Eng. Struct. **86**, 122–133 (2015)

Liu, J., Liao, C., Jin, H., Jiang, Z., Zhong, D., Tang, L.: Numerical model of the effect of water vapor environment on the chloride transport in concrete. Constr. Build. Mater. **311**, 125330 (2021)

Liu, Q.-F., Shen, X.-H., Šavija, B., Meng, Z., Tsang, D.C.W., Sepasgozar, S., Schlangen, E.: Numerical study of interactive ingress of calcium leaching, chloride transport and multi-ions coupling in concrete. Cem. Concr. Res. **165**, 107072 (2023a)

Liu, Q.F., Cai, Y.X., Peng, H., Meng, Z.Z., Mundra, S., Castel, A.: A numerical study on chloride transport in alkali-activated fly ash/slag concretes. Cem. Concr. Res. **166**, 107094 (2023b)

Meijers, S.J.H., Bijen, J.M.J.M., de Borst, R., Fraaij, A.L.A.: Computational results of a model for chloride ingress in concrete including convection drying-wetting cycles and carbonation. Mater. Struct. **38**(276), 145–154 (2005)

Mercado-Mendoza, H., Lorente, S., Bourbon, X.: The diffusion coefficient of ionic species through unsaturated materials. Transp. Porous Med. **96**(3), 469–481 (2013)

Meng, Z.Z., Liu, Q.F., Ukrainczyk, N., Mu, S., Zhang, Y.F., Schutter, G.D.: Numerical study on the chemical and electrochemical coupling mechanisms for concrete under combined chloride-sulfate attack. Cem. Concr. Res. (2024)

Millington, R., Quirk, J.: Permeability of porous solids. Trans. Faraday Soc. **57**, 1200–1207 (1961)

Monlouis-Bonnaire, J.P., Verdier, J., Perrin, B.: Prediction of the relative permeability to gas flow of cement-based materials. Cem. Concr. Res. **34**(5), 737–744 (2004)

Na, O., Xi, Y.P.: Parallel finite element model for multispecies transport in nonsaturated concrete structures. Materials **12**(17), 2764 (2019)

Nielsen, E.P., Geiker, M.R.: Chloride diffusion in partially saturated cementitious material. Cem. Concr. Res. **33**(1), 133–138 (2003)

Oh, B.H., Jang, S.Y.: Effects of material and environmental parameters on chloride penetration profiles in concrete structures. Cem. Concr. Res. **37**(1), 47–53 (2007)

Patel, R.A., Churakov, S.V., Prasianakis, N.I.: A Multi-level pore scale reactive transport model for the investigation of combined leaching and carbonation of cement paste. Cem. Concr. Compos. **115**, 103831 (2021)

Saetta, A.V., Scotta, R.V., Vitaliani, R.V.: Analysis of chloride diffusion into partially saturated concrete. ACI Mater. J. **90**(5), 441–451 (1993)

Samson, E., Marchand, J.: Modeling the transport of ions in unsaturated cement-based materials. Comput. Struct. **85**(23–24), 1740–1756 (2007)

Samson, E., Marchand, J., Snyder, K.A., Beaudoin, J.J.: Modeling ion and fluid transport in unsaturated cement systems in isothermal conditions. Cem. Concr. Res. **35**(1), 141–153 (2005)

Savija, B., Lukovic, M., Schlangen, E.: Lattice modeling of rapid chloride migration in concrete. Cem. Concr. Res. **61–62**, 49–63 (2014)

Singla, A., Savija, B., Sluys, L.J., Rodriguez, C.R.: Modelling of capillary water absorption in sound and cracked concrete using a dual-lattice approach: computational aspects. Constr. Build. Mater. **320**, 125826 (2022)

Song, H.W., Lee, C.H., Ann, K.Y.: Factors influencing chloride transport in concrete structures exposed to marine environments. Cem. Concr. Compos. **30**(2), 113–121 (2008)

Tang, L.P.: Engineering expression of the clinconc model for prediction of free and total chloride ingress in submerged marine concrete. Cem. Concr. Res. **38**(8–9), 1092–1097 (2008)

Tang, L.P., Gulikers, J.: On the mathematics of time-dependent apparent chloride diffusion coefficient in concrete. Cem. Concr. Res. **37**(4), 589–595 (2007)

Tang, L.P., Nilsson, L.-O.: Chloride binding capacity and binding isotherms of opc pastes and mortars. Cem. Concr. Res. **23**(2), 247–253 (1993)

Thiery, M., Belin, P., Baroghel-Bouny, V. Nguyen, M. D. (2013), Modeling of isothermal drying process in cementitious materials, IN: Thermo-Hydromechanical and Chemical Coupling in Geomaterials and Applications, pp. 571–579.

Tong, L.Y., Xiong, Q.X., Zhang, M.Z., Meng, Z.Z., Meftah, F., Liu, Q.F.: Multi-scale modelling and statistical analysis of heterogeneous characteristics effect on chloride transport properties in concrete. Constr. Build. Mater. **367**, 130096 (2023)

Tong, L.Y., Xiong, Q.X., Ke, X., et al.: Advanced modelling of moisture transport features in unsaturated cementitious materials considering multimodal pore size distribution. Mater. Struct. (2024a)

Tong, L.Y., Xiong, Q.X., Zhang, Z., et al.: A novel lattice model to predict chloride diffusion coefficient of unsaturated cementitious materials based on multi-typed pore structure characteristics. Cem. Concr. Res. 107351 (2024b)

Ukrainczyk, N., Koenders, E.A.B.: Representative elementary volumes for 3d modeling of mass transport in cementitious materials. Modell. Simul. Mater. Sci. Eng. **22**(3), 035001 (2014)

Van Genuchten, M.T.: A closed-form equation for predicting the hydraulic conductivity of unsaturated soils. Soil Sci. Soc. Am. J. **44**(5), 892–898 (1980)

Wang, P.G., Jia, Y.T., Li, T., Hou, D.S., Zheng, Q.: Molecular dynamics study on ions and water confined in the nanometer channel of Friedel's salt: structure dynamics and interfacial interaction. Phys. Chem. Chem. Phys. **20**(42), 27049–27058 (2018)

Wong, S.F., Wee, T.H., Swaddiwudhipong, S., Lee, S.L.: Study of water movement in concrete. Mag. Concr. Res. **53**(3), 205–220 (2001)

Xiong, Q.X., Tong, L.Y., Meftah, F., et al.: Improved Predictions of Permeability Properties in Cement-based Materials: A Comparative Study of Pore Size Distribution-based Models. Constr. Build. Mater. (2024)

Xiong, Q.X., Tong, L.Y., Zhang, Z.D., Shi, C.J., Liu, Q.F.: A new analytical method to predict permeability properties of cementitious mortars: the impacts of pore structure evolutions and relative humidity variations. Cem. Concr. Compos. **137**, 104912 (2023)

Yang, Y.K., Patel, R.A., Churakov, S.V., Prasianakis, N.I., Kosakowski, G., Wang, M.: Multiscale modeling of ion diffusion in cement paste: electrical double layer effects. Cem. Concr. Compos. **96**, 55–65 (2019)

Zhang, Z.D., Angst, U.: A dual-permeability approach to study anomalous moisture transport properties of cement-based materials. Transp. Porous Media **135**(1), 59–78 (2020)

Zhang, J., Gao, Y., Han, Y.D., Sun, W.: Shrinkage and interior humidity of concrete under dry-wet cycles. Dry. Technol. **30**(6), 583–596 (2012)

Zhang, M.Z., Ye, G., van Breugel, K.: Multiscale Lattice Boltzmann-finite element modelling of chloride diffusivity in cementitious materials part I: algorithms and implementation. Mech. Res. Commun. **58**, 53–63 (2014)

Zhang, Z.D., Thiery, M., Baroghel-Bouny, V.: Investigation of moisture transport properties of cementitious materials. Cem. Concr. Res. **89**, 257–268 (2016)

Zhang, P., Wittmann, F.H., Vogel, M., Muller, H.S., Zhao, T.J.: Influence of freeze-thaw cycles on capillary absorption and chloride penetration into concrete. Cem. Concr. Res. **100**, 60–67 (2017)

Zhang, P., Wittmann, F.H., Lura, P., Muller, H.S., Han, S.B., Zhao, T.J.: Application of neutron imaging to investigate fundamental aspects of durability of cement -based materials: a review. Cem. Concr. Res. **108**, 152–166 (2018)

Zhang, C.L., Chen, W.K., Mu, S., Savija, B., Liu, Q.F.: Numerical investigation of external sulfate attack and its effect on chloride binding and diffusion in concrete. Constr. Build. Mater. **285**, 122806 (2021)

Zhao, K.Y., Qiao, Y., Zhang, P., Bao, J.W., Tian, Y.P.: Experimental and numerical study on chloride transport in cement mortar during drying process. Constr. Build. Mater. **258**, 119655 (2020)

Zhou, C.S.: General solution of hydraulic diffusivity from sorptivity test. Cem. Concr. Res. **58**, 152–160 (2014)